Sensorless Speed Control of PMSM in Low-Speed by High Frequency Pulsating Injection with Double Modulation Error Compensation

Indra Ferdiansyah[1*], and *Tsuyoshi Hanamoto*[1]

[1]Kyushu Institute of Technology, Department of Life Science and Systems Engineering, Fukuoka, 808-0196, Japan

Abstract. A novel improvement scheme for the High Frequency Pulsating Injection-Sinusoidal (HFPI-S) method that considers the error function is proposed and implemented for PMSM sensorless control. The limitations in extracting the error function and dealing with signal noise at low-speed could appear the estimation errors in rotor position within the HFPI-S system. In this study, a new model for the proposed method, including the addition of dual modulation as error compensation in the process of extracting rotor position and enhancing the observer for conventional rotor position signals was focused. The results of this study showed that the extraction of the error function that is expanded could obtain more accurate results. Therefore, the addition of dual modulation and the observer enhancement could be effectively applied to maintain the accuracy of rotor position estimation even under low-speed and loaded conditions.

1 Introduction

Permanent magnet synchronous motors (PMSM) have been widely applied in industry, especially in electric vehicles, home appliances and robots, due to their high efficiency and high torque density [1-3]. In earlier report, the common procedure to obtain accurate rotor position information used in designing high-performance PMSM drive systems is electromechanical sensors [4]. However, these sensors not only reduces the mechanical robustness of the drive system, but also increases cost, size, weight and cabling complexity [5]. Therefore, the techniques without position sensors play an important role in practical applications as an alternative to mechanical sensors [6-8].

Sensorless control techniques can be divided into two categories, namely fundamental model or observer and saliency based methods [6], [9-10]. Fundamental model or observer based methods are model that effective at medium and high speed ranges. Meanwhile, salience-based methods are effective at low speeds. The first category of the method estimates position-related states, such as the back electromagnetic force (EMF) because its amplitude is proportional to the rotor speed, so that the rotor position information can be extracted [11]. However, this category method is in low performance or even fail in the low-speed region due to the back EMF amplitude is too small. Meanwhile, the second category method, which

* Corresponding author: ferdiansyah.indra986@mail.kyutech.jp

are particularly effective at low speeds, exploit the anisotropic properties of the machine, such as rotor salience and or stator iron saturation [12]. The position estimation of rotor can be performed by applying the high frequency sinusoidal injection pulsating and rotating method. In addition, the sinusoidal and square waves was reported to be effective as the injected carrier signal [6]. The second category method, a high-frequency voltage signal is injected into the PMSM. Due to the saliency effect in the PMSM, the corresponding high-frequency current response is modulated to obtain the rotor position information [8],[12]. In this paper, the double modulation HFPI-S method with error compensation is described as a solution to the limitations in rotor position extraction of general HFPI-S systems in previous work [8]. In addition, the difference between the actual rotor position and the estimated rotor position value caused by high-frequency injection in the rotor position extraction process is described as $\Delta\theta$. The modulation technique is used to obtain the rotor position information through the $\Delta\theta$ function. In this context, the accuracy of the rotor position extraction results is highly dependent on the characteristics of the signal. However, at low speed of the motor together with their changes, the present other signals such as torque ripple and transient condition might affect the performance of system. Moreover, the system could affect the $\Delta\theta$ function due to the signal modulation of the system is performed on quadrature currents. Therefore, error compensation of this function is proposed as a solution to increase the extraction yield of the rotor position. In addition, it should be noted that general systems only modulate half of the signal, so that error compensation is also applied in the extraction process to improve the accuracy of the resulting rotor position information.

2 Mathematical Model of PMSM

The PMSM equation of voltage can be expressed in the d and q reference frames as follows:

$$\begin{bmatrix} v_d \\ v_q \end{bmatrix} = \begin{bmatrix} R & -\omega_r L_q \\ \omega_r L_d & R \end{bmatrix} \begin{bmatrix} I_d \\ I_q \end{bmatrix} + \begin{bmatrix} L_d & 0 \\ 0 & L_q \end{bmatrix} p \begin{bmatrix} I_d \\ I_q \end{bmatrix} + \begin{bmatrix} 0 \\ \omega_r \varphi_f \end{bmatrix} \quad (1)$$

Where v_d, v_q, i_d, i_q, R, L_d, L_q are the stator voltage in d-q axis, the current voltage in d-q axis, resistance of the motor and the inductances in d-q axis, respectively, meanwhile p, ω_r, φ_f are $\frac{d}{dt}$, rotational speed of the motor and the permanent linkage of the motor, respectively.

In low-speed condition, the back EMF and the cross-coupling corelated to Eq (1) that can be neglected. Therefore, the equation of PMSM can be simplified as follows:

$$\begin{bmatrix} v_d \\ v_q \end{bmatrix} = \begin{bmatrix} R & 0 \\ 0 & R \end{bmatrix} \begin{bmatrix} I_d \\ I_q \end{bmatrix} + \begin{bmatrix} L_d & 0 \\ 0 & L_q \end{bmatrix} p \begin{bmatrix} I_d \\ I_q \end{bmatrix} \quad (2)$$

In this study, the stator resistance is smaller than stator inductance due to the high frequency signal injection. Hence, the PMSM equation can be written as follows:

$$\begin{bmatrix} v_d \\ v_q \end{bmatrix} = \begin{bmatrix} L_d & 0 \\ 0 & L_q \end{bmatrix} p \begin{bmatrix} I_d \\ I_q \end{bmatrix} \quad (3)$$

Because the relationship of rotor position in d-q axis could not be directly described. Therefore, α-β stationary reference frame is needed, as shown in the correlation of Fig. 1.

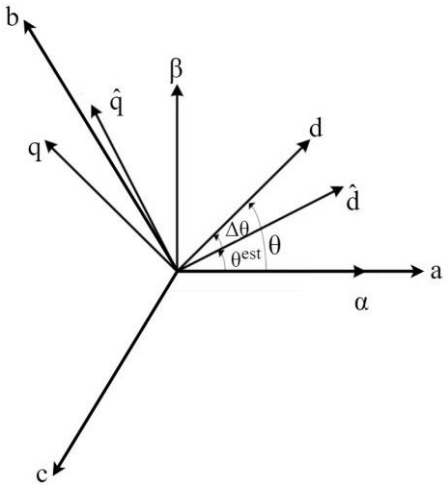

Fig. 1. The relationship of rotor position among three reference frames.

The basic concept of PMSM sensorless motor control using high frequency pulsating injection adjusts the $\Delta\theta$ closet to zero, while in Clarke transformation a phase winding is align to α-axis. So that in the d-q axis reference frame, the electrical angle between α-axis and d-axis is θ. The estimated axis is denoted as $\hat{d}-\hat{q}$ axis reference frame, then the electrical angle between α-axis and $\hat{d}$-axis is θ^{est}. So that the estimated error can be written as below:

$$\Delta\theta = \theta - \theta^{est} \tag{4}$$

By some modulation techniques, the information related to the $\Delta\theta$ can be obtained. In addition, to obtain the position of the rotor, the θ^{est} should be actual to actual position. Therefore, the closed-loop systems in this study the $\Delta\theta$ was adjusted to go to zero.

3 Proposed high-frequency pulsating injection sinusoidal with double modulation error compensate

Based on the high frequency pulse injection principle, the $\Delta\theta$ can be extracted to obtain rotor position information through the correlation of the equation function in the actual coordinate system. The estimated coordinate can be expressed in the Eq. (5) as follows:

$$F_{act-est} = \begin{bmatrix} \cos(\Delta\theta) & -\sin(\Delta\theta) \\ \sin(\Delta\theta) & \cos(\Delta\theta) \end{bmatrix} \tag{5}$$

In accordance (3), a sinusoidal pulsating voltage is injected into the estimated d-q rotating reference frame that can be described by the following equation:

$$v^i = \begin{bmatrix} v_{\hat{d}} \\ v_{\hat{q}} \end{bmatrix} = u_{inj} \begin{bmatrix} \cos(\omega_{inj} t) \\ 0 \end{bmatrix} \tag{6}$$

Where u_{inj} and ω_{inj} are the amplitude and frequency of the injected voltage, respectively. To project the $\hat{d}-\hat{q}$ axis on the d-q axis, the resulting voltage in d-q_h can be expressed as follows:

$$vd,q_h = (v^i)(F_{act-est}) = v^i \begin{bmatrix} \cos(\Delta\theta) \\ -\sin(\Delta\theta) \end{bmatrix} \tag{7}$$

By combining (3) and (7), the equation can be obtained as follows:

$$p\begin{bmatrix} i_{d,h} \\ i_{q,h} \end{bmatrix} = F_{act-est}\begin{bmatrix} \frac{1}{L_{dh}} & 0 \\ 0 & \frac{1}{L_{qh}} \end{bmatrix}\begin{bmatrix} v_{d,h} \\ v_{q,h} \end{bmatrix} \tag{8}$$

Finally the current in d-q$_{,h}$ can be express as follows:

$$id_h = \int \frac{v^i \cos(\Delta\theta)}{Ld_h} dt = \frac{u_{inj} \sin(\omega_{inj} t)\cos(\Delta\theta)}{Ld_h \omega_{inj}} \tag{9}$$

$$iq_h = \int \frac{v^i \sin(\Delta\theta)}{Lq_h} dt = \frac{u_{inj} \sin(\omega_{inj} t)\sin(\Delta\theta)}{Lq_h \omega_{inj}} \tag{10}$$

The relationship between current and voltage in the estimated $\hat{d}-\hat{q}$ two-phase rotating reference frame from (6) and (8). In addition, when the high frequency injected in $\hat{d}$-axis, the position information can be extracted from the induced current signal in the estimated rotating reference frame as shown in the below equation:

$$\begin{bmatrix} \hat{v_{d,h}} \\ \hat{v_{q,h}} \end{bmatrix} = \frac{u_{inj} \sin(\omega_{inj} t)}{\omega_{inj} L_{dh} L_{qh}} \begin{bmatrix} L_{qh}\cos^2\Delta\theta + L_{dh}\sin^2\Delta\theta \\ \frac{\sin(2\Delta\theta)}{2}(L_{qh} - L_{dh}) \end{bmatrix}$$
$$\hat{i_{d,h}} = (k_1 + k_2\cos(2\Delta\theta))\sin(\omega_{inj} t)$$
$$\hat{i_{q,h}} = k_2 \sin(2\Delta\theta)\sin(\omega_{inj} t) \tag{11}$$

Where $k1$ and $k2$ are expressed in the below equation:

$$k_1 = \frac{u_{inj}(L_{qh} + L_{dh})}{2\omega_{inj} L_{dh} L_{qh}}, k_2 = \frac{u_{inj}(L_{qh} - L_{dh})}{2\omega_{inj} L_{dh} L_{qh}} \tag{12}$$

In general, Fig. 2(a) describe that when signal injection is used in the $\hat{d}$ -axis, the position estimation error $\Delta\theta$ of the rotor can be obtained by detecting the current effect in the $\hat{q}$-axis as well as by applying appropriate processing to the current signal. Therefore, the amplitude of the $\hat{\imath q}$ ($iamp$) can be extracted by signal modulation as follows:

$$i_{amp} = iq_{,h}^{\wedge} \sin(\omega_{inj} t) \tag{13}$$

A bandpass filter (BPF) is also possible to be added before multiplying the amplitude of current signal (i_{amp}) by the injected modulation $\{\sin(\omega_{inj} t)\}$. Then, the multiplication results were pass through a low-pass filter (LPF) to extract DC component. So that, the output current containing the error of rotor position estimation can be obtained in the below equation:

$$f\Delta\theta = LPF\left[iq_{,h}^{\wedge} \sin(\omega_{inj} t)\right] = k_3 \sin(2\Delta\theta) \tag{14}$$

Where $k3$ as follows,

$$k_3 = \frac{1}{2} k_2 = \frac{u_{inj}(L_{qh} - L_{dh})}{4\omega_{inj} L_{dh} L_{qh}} \tag{15}$$

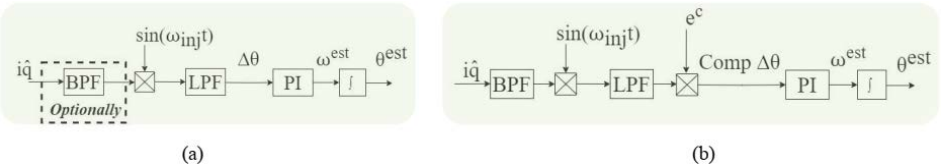

Fig. 2. Extraction of rotor position in sensorless HFPI-S. (a) rotor position extraction in general, (b) rotor position extraction with error compensation.

In Eq. 14, it is important to note that the amplitude of the error signal is only half and the linearization of the sinusoidal term in $\Delta\theta$ is needed.

An outline of the proposed scheme of rotor position extraction is shown in Fig. 2(b). A BPF was added in the d-q- axis rotating frame to extract high- frequency current signal and maintain current signal from another signal effect in low-speed condition. In addition, LPF was used after multiplying the current signal by the injected modulation $\{\sin(\omega inj t)\}$. The error term was compensated based on the estimated error amplitude and linearization of sinusoidal term was implemented to fine-tune the position tracking,

In addition, the term compensation was used to expand the information about the error that control by the Proportional-Integral (PI) controller to reach Δθ equal to 0. The error compensation by double modulation is expressed as follows:

$$e^c = \left|\frac{1}{2k_3}\right| = \left|\frac{2\omega L_d L_q}{u_{inj}^{ec}(L_q - L_d)}\right| \tag{16}$$

Furthermore, to achieve optimal estimation results, information regarding $\Delta\theta$ in the case of change in speed, the addition of loads, or other conditions such as the effects of signal noise in low-speed are needed to maintain the extraction of rotor position estimates in good results. The compensation will be provided through the response of changes indicated by variable ω within the system to ensure the estimated rotor position can obtain more accurate results.

4 Simulation result

Based on the analysis above mentioned, the block of diagram proposed system can be seen in Fig 3. Subsequently, a model in SIMULINK MATLAB was built and simulated. The parameter simulation of PMSM used in this study are shown in TABLE 1.

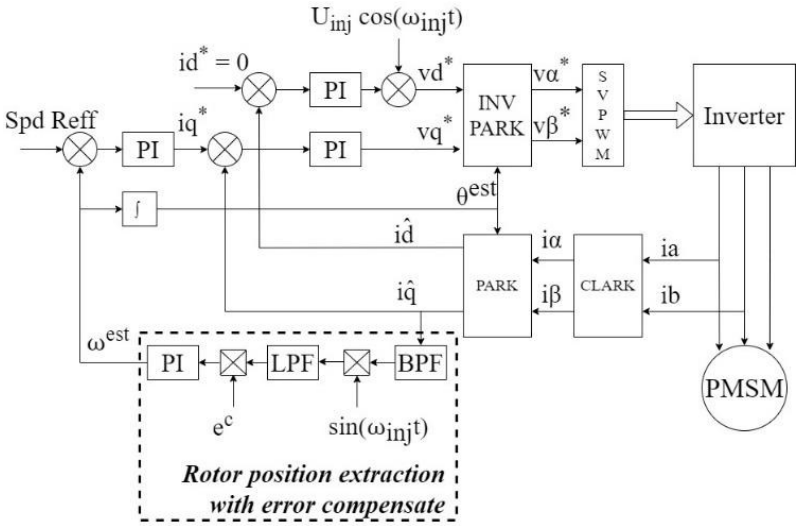

Fig. 3. The overall proposed scheme.

Table 1. Simulation parameter of PMSM.

Parameter	Value	Parameter	Value
DC Bus Voltage (V)	60	Flux (Wb)	0.446
Stator Resistance (Ω)	1.1	Moment of Inertia (kgm2)	0.077
d-Axis Inductance (H)	0.0057	Viscous Damping (Nms)	0.009
q-Axis Inductance (H)	0.0077	Pole of Pairs	2

In order to evaluate the dynamic performance of the HFPI-S- double modulation with error compensate-based position estimation, simulation tests were conducted with low-speed variations. The experimental results of these tests are shown in Fig 4 and Fig 5, respectively. The first test was carried out by setting the speed reference value of 25 min^{-1}. The speed reference value is increased to 75 min^{-1} after 0.5 seconds to observe the response of the proposed system. In Fig 4, it can be seen that the control system functions work properly in reaching both speed reference values within 0.3 seconds. In addition, it was found that during dynamic conditions, the system is able to maintain the rotor position estimation error below 10 el.deg.

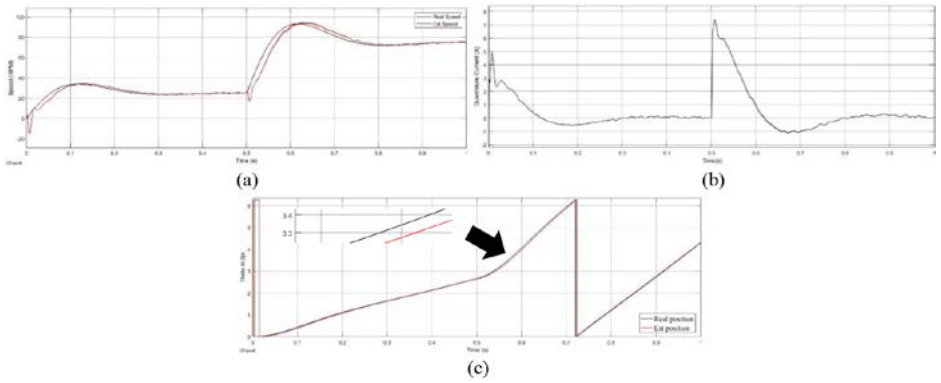

Fig. 4. Response of systems under a steep speed from 25min^{-1} to 75min^{-1}. (a) rotor speed, (b) q-axis current, (c) rotor position.

The variation of speed reference value was applied in the second test by starting with an initial value of 80 min^{-1}. In this test, the speed was decreased to 40 min^{-1} after 0.5 seconds. The result exhibited that system is able to operate optimally and could reach the speed reference value of 0.45 seconds for 80 min^{-1} and 0.25 seconds for 40 min^{-1} with an estimation error of the rotor position not exceeding 5 el.deg. The details of the simulation results are shown in Fig 5.

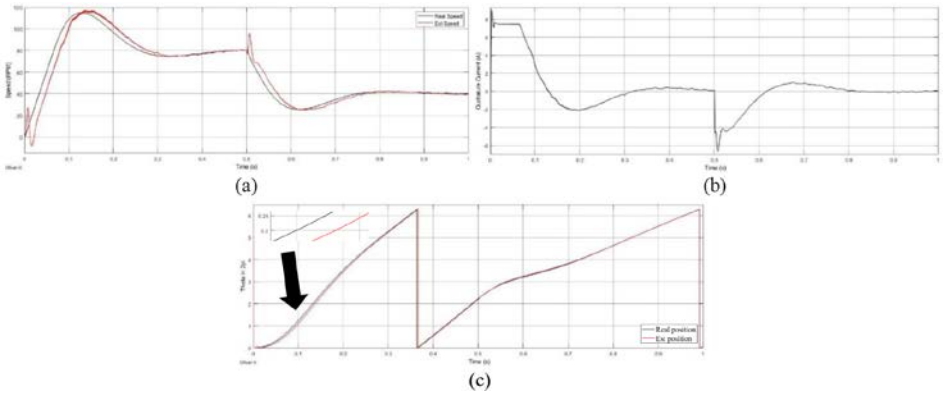

Fig. 5. Response of systems under a steep speed from 80min^{-1} to 40min^{-1}. (a) rotor speed, (b) q-axis current, (c) rotor position.

In the third simulation test, the system was performed under load conditions. In this case, the speed reference value is made to constant at 30 min^{-1}, the motor was given a load of 3 Nm after 0.55 seconds. The obtained results (Fig.6) showed that the system can operate properly and could maintain the speed according to the given speed reference values. In this simulation, it seems to decrease when the motor is loaded. However, the systems could return to the speed according to the speed reference value in less than 0.3 seconds. Furthermore, during these dynamic conditions, the rotor position estimation error also did not exceed of 5 el.deg.

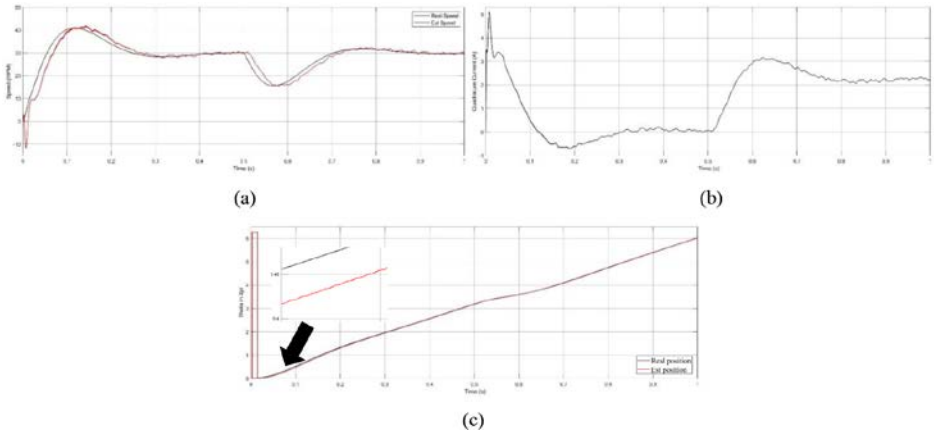

Fig. 6. Response of systems under a speed 30min^{-1} and constant load torque 3Nm. (a) rotor speed, (b) q-axis current, (c) rotor position.

The last test on this system was conducted by applying two-speed reference values, namely from a negative value to a positive value. This test is intended to demonstrate that the proposed sensorless control system can operate optimally, regardless of the motor rotation direction.

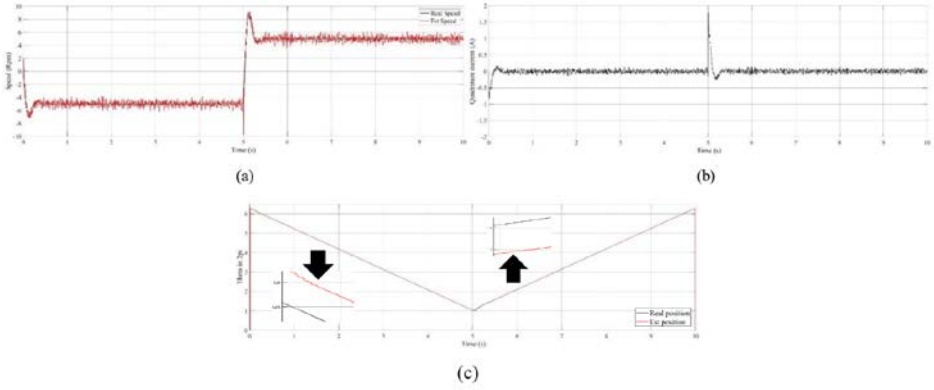

Fig. 7. Response of systems under a minus and positive value of speed references -5 min^{-1} and 5 min^{-1}. (a) rotor speed, (b) q-axis current, (c) rotor position.

In Fig. 7, it can be seen that the system is able to operate effectively in both directions with time that reach the speed reference value of less than 0.5 seconds and the estimated rotor position error below 5 el.deg in conditions of -5 min^{-1} and 5 min^{-1}. Therefore, the proposed control system is not only suitable for use in one motor rotation direction, but also applicable to both rotation directions.

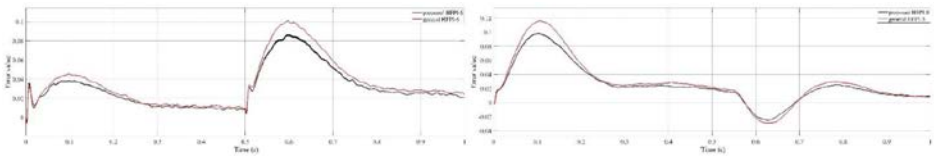

(a) (b)

Fig. 8. Comparison of the rotor position error value between the proposed and general systems. (a) under change speed condition, (b) under loaded condition.

In comparison between general and proposed systems in this study (Fig 8), it seems to indicate that the proposed system error values were small than that of the general systems. Therefore, the proposed systems from this study could be aplied in sensorless PMSM motor control especiely ini low-speed area and dynamic condition.

5 Conclusion

In this paper, the high frequency pulsating injection sinusoidal with double modulation error compensate method for sensorless control at low speeds has been elaborated and evaluated. Several dynamic tests were conducted to assess the performance of systems reliability. The tests included variations in low speed and load addition with control responses that capable to reach the reference speed values with minimal ripple and lower rotor position estimation error. Based on simulation results, the designed sensorless control strategy for an PMSM can track the real rotor position accurately and exhibit optimal control responses in dynamic conditions in low-speed range. Moreover, the proposed system could also be implemented for both directions of motor rotation (clockwise or counter-clockwise). Therefore, the designed control system did not require initial settings to change the motor rotation direction. To verify the proposed method at extremely low-speed below 5 min^{-1} by minimizing system overshoot and conducting experimental verification using an actual motor is needed in the future work.

References

1. S. Wang, K. Yang and K. Chen, An Improved Position-Sensorless Control Method at Low Speed for PMSM Based on High-Frequency Signal Injection into a Rotating Reference Frame. IEEE Access, 2019, pp. 86510 - 86521.
2. A. Benevieri, A. Formentini, Marchesoni, M. Passalacqua and L. Vaccaro, Sensorless Control with Switching Frequency Square Wave Voltage Injection for SPMSM with Low Rotor Magnetic Anisotropy. IEEE Transactions on Power Electronics, 2023, pp. 10060 – 10072.
3. B. Han, Y. Shi, X. Song, K. Hong and K. Mao, Initial Rotor Position Detection Method of SPMSM based On New High Frequency Voltage Injection Method. IEEE Transactions on Power Electronics, 2018, pp. 3553 – 3562.
4. W. Yang, H. Guo, X. Sun, Y. Wang, S. Riaz and H. Zaman, Wide-Speed-Range Sensorless Control of IPMSM. Electronics, 2022, pp. 1-19.
5. S. Maekawa, M. Wu and H. Kubota, Position Sensorless Control Method for Permanent Magnet Synchronous Motor Using Speed Observer and Opened Phase Voltage Caused by Magnetic Saliency. IEEJ Journal of Industry Applications,2019, pp. 875 – 883.

6. G. Wang, M. Valla and J. Solsona, Position Sensorless Permanent Magnet Synchronous Machine Drives—A Review. IEEE Transactions on Industrial Electronics, 2019, pp. 5830 - 5842.
7. R. Hosooka and S. Shinnaka, New sensorless vector control of PMSM by discrete-time voltage injection of PWM carrier frequency- High-frequency current correlation method, *in 2017 IEEE 12th International Conference on Power Electronics and Drive Systems*, IEEE Conference Publications. (The Institute of Electrical and Electronics Engineers, Honolulu, HI, USA, 2017) pp. 913-918.
8. H. Wang, G. Deng, X. Wu and S. Huang, Comparison Between High Frequency Sinusoidal Pulsating Voltage and Minimum-Voltage Vector Injection for Sensorless Control of PMSM Drives, in *2019 22th International Conference on Electrical Machines and Systems*, IEEE Conference Publications. (The Institute of Electrical and Electronics Engineers, Harbin, China, 2019) pp. 1-6.
9. H. Zhang, G. Zhang, W. Shen, G. Wang and D. Xu, Fundamental PWM Excitation Based Low-Speed Sensorless Control Method for PMSM Drives, in *2020 15th IEEE Conference on Industrial Electronics and Applications*, IEEE Conference Publications. (The Institute of Electrical and Electronics Engineers, Kristiansand, Norway, 2020) pp. 833-838.
10. D. Hirakawa, K. Yamamoto and A. Shinohara, Estimated Position Error Compensation Method Taking Impact of Load and Speed into Account in PMSM Position Sensorless Control Based on High Frequency Voltage Injection, in *2020 23rd International Conference on Electrical Machines and Systems*, IEEE Conference Publications. (The Institute of Electrical and Electronics Engineers, Hamamatsu, Japan, 2020) pp. 246-251.
11. W. Li, M. Wu, X. Huang and Z. Li, Improved High Frequency Signal Injection Method Based on Fundamental Current Extraction for Permanent Magnetic Synchronous Motors, in *2021 IEEE 30th International Symposium on Industrial Electronics*, IEEE Conference Publications. (The Institute of Electrical and Electronics Engineers, Kyoto, Japan, 2021) pp. 01-06.
12. K. Rehorik, B. Grothman, A. Elsman, D. Gerling and F. Capponi, Compensation of Saliency Tracking Static Estimation Errors in Sensor Fault Tolerant IPMSM Drives, in *IECON 2020 The 46th Annual Conference of the IEEE Industrial Electronics Society*, IEEE Conference Publications. (The Institute of Electrical and Electronics Engineers,Singapore, 2020) pp. 901-906.